Scaling properties of delay times in one-dimensional random media

Joshua D. Bodyfelt,[1] J. A. Méndez-Bermúdez,[2] Andrey Chabanov,[3] and Tsampikos Kottos[1]
[1]*Department of Physics, Wesleyan University, Middletown, Connecticut 06459, USA*
[2]*Instituto de Física, Universidad Autónoma de Puebla, Apartado Postal J-48, Puebla 72570, Mexico*
[3]*Department of Physics and Astronomy, The University of Texas at San Antonio, Texas 78249, USA*
(Received 29 August 2007; published 3 January 2008)

The scaling properties of the inverse moments of Wigner delay times are investigated in finite one-dimensional (1D) random media with one channel attached to the boundary of the sample. We find that they follow a simple scaling law which is independent of the microscopic details of the random potential. Our theoretical considerations are confirmed numerically for systems as diverse as 1D disordered wires and optical lattices to microwave waveguides with correlated scatterers.

DOI: 10.1103/PhysRevB.77.045103 PACS number(s): 72.15.Rn, 72.20.Dp, 73.23.−b

I. INTRODUCTION

The study of the statistical properties of Wigner delay times has been a subject of intense research activity.[1–14] The Wigner delay time is defined as the energy derivative of the total phase of the scattering matrix S, i.e., $\tau_W = -i\hbar\partial \ln \det S/\partial E$, and can be interpreted as a time delay in propagation of the peak of the wave packet due to scattering interference, in comparison to a free wave packet propagation. Although most of the contemporary activity has been focused in understanding the statistical properties of delay times within chaotic mesoscopic systems,[1,2] recently the interest has shifted toward random scattering media exhibiting Anderson localization[3–11] including the most difficult case of the Anderson metal-insulator transition.[10–14] On the experimental side,[3–5] the statistics of scattering phases and delay times have been measured in microwave experiments with quasi-one-dimensional random samples, while on the theoretical side, the main effort has been to connect the statistical properties of delay times with that of eigenfunctions.[10–13] Establishing such a relation may open new exciting opportunities for measuring the statistical properties of eigenfunctions[15–24] via the experimentally accessible delay times.

Specifically, using the powerful nonlinear σ model (NLσM) technique,[11,12] an exact relation was found linking the probability distribution of eigenfunction components within a random medium to the distribution of Wigner delay times in the same sample of length L, with one channel attached at its bulk. This relation is *exact on the level of the* NLσM and valid independent of the system size L (i.e., irrespective if we take the thermodynamic limit $L\to\infty$ or keep L finite).

However, one has to question the validity of mapping a particular microscopic model of a disordered system onto the NLσM. More specifically, this mapping is approximately correct in the case of weak disorder and breaks down totally for strong disorder. Another strict requirement is that the underlying geometry allows for a diffusive process—this certainly is not the case for strictly one-dimensional (1D) random media. Finally, NLσM calculations preassume that the disorder potential is white noise, thus excluding the emerging family of disordered systems with imprinted correlations in their potential.[25–32] The above restrictions cast reasonable doubts on the validity of NLσM predictions, as far as *realistic* systems are concerned, and call for testing by means of a dedicated experiment or computer simulation.

It is the purpose of this paper to investigate the scaling properties of moments of delay times and compare them with the ones found for wave functions in cases where the conditions for NLσM applicability are violated. To this end, we will study various microscopic systems: (a) a 1D disordered electronic system (modeled by an Anderson Hamiltonian), (b) a microwave system with long-range correlated scatterers inside a waveguide (modeled by a Kronig-Penney model), and (c) cold atoms in a disordered optical lattice (modeled again by a Kronig-Penney model with binary distribution). In all cases, we find that the inverse moments of delay times τ_L in a disordered sample of length L follow a simple scaling law which is independent of the microscopic properties belonging to the underlying physical system. Specifically, we find that

$$\beta_{-q} = f(\lambda_{-q}), \quad \beta_{-q} \equiv \frac{\tau_{\mathrm{ref}}^{-q}}{\langle \tau_L^{-q} \rangle}, \quad \lambda_{-q} \equiv \frac{\tau_{\mathrm{ref}}^{-q}}{\langle \tau_\infty^{-q} \rangle}, \tag{1}$$

where q takes positive values and $\langle \tau_L \rangle$ represents the average (or typical) delay time over disorder realizations. The variable τ_∞ represents the delay time of the $L\to\infty$ sample with the same disordered potential. The variable τ_{ref} is the delay time of a "reference" sample, corresponding to an "infinite" localization length setup, with length L. The former quantity incorporates the microscopic information of the system (i.e., disorder potential), whereas τ_{ref} only depends on the information of the finite sample length L, as well as the dimensionality and the energy E at which the scattering experiment is performed. Our numerical analysis indicates that the scaling law [Eq. (1)] can take the model-independent form,

$$\langle \tau_L^{-q}(\epsilon, E) \rangle = \langle \tau_\infty^{-q}(\epsilon, E) \rangle + \tau_{\mathrm{ref}}^{-q}, \tag{2}$$

where ϵ is the disorder strength of the random potential. In fact, our numerical data suggest that Eq. (2) is exact only for $q=1$, while for higher q values, small deviations from the linear behavior can be detected.

We point out that a similar relation to Eq. (2) was found for the scaling properties of wave function moments within a closed disordered sample.[15–17] The corresponding expression involves the $q'=q+1$ wave function moment and reads

$$\frac{1}{\langle l_L^{(q')}(\epsilon,E)\rangle} = \frac{1}{\langle l_\infty^{(q')}(\epsilon,E)\rangle} + \frac{1}{l_{\rm ref}^{(q')}}, \tag{3}$$

where $l_L^{(q')}=L(P^{(q')}/P_{\rm ref}^{(q')})^{1/(1-q')}$ are the various information lengths of a sample with length L, $P^{(q')}\equiv\Sigma_n^L|\psi_n|^{2q'}$ with eigenfunction components ψ_n, $l_\infty(\epsilon,E)$ is the localization length of the infinite sample with the same disordered strength, and $P_{\rm ref}^{q'}\sim L$ with a prefactor defined by the reference geometry (1D periodic lattice in the cases studied here). For the special case $q'=1$, the corresponding information length is equal to the entropic length defined by $l_L^{(1)}=e/2\,\exp(-\Sigma_{n=1}^L|\psi_n|^2\ln|\psi_n|^2)$.

We initiate our analysis by recalling the notion of delay times as originally proposed by Wigner and de Carvalho and Nussenzveig.[35,36] This is the time that a reflected particle is delayed due to interaction with a scattering region. Now, we recall that the $q'=2$ information length, $l_L^{(2)}(\epsilon,E)$, (associated with the inverse participation ratio) measures the "penetration" (localization) length inside a disordered sample before the particle is reflected back (we are considering here the one channel scattering setup). The corresponding delay time due to the scattering from the disordered sample is then given by $\tau_L=2l_L^{(2)}/v$, where v is the group velocity of the wave packet centered around energy E. Using this argument and substituting it for $l_L^{(2)}$ in Eq. (3), we obtain Eq. (2) for $q=1$. In fact, our numerical data (see below) indicate that Eq. (2) describes to a good approximation higher q moments as well.

Below, we report our numerical results for various microscopic models which support the scaling of Eq. (1). Although our presentation focuses on the first moment $q=1$, we have found that higher moments follow the scaling law [Eq. (1)] equally well.

II. MICROSCOPIC MODELS AND UNIVERSALITY

A. 1D disordered electronic system

The standard model that describes a 1D disordered electronic sample is the tight-binding equation,

$$\psi_{n+1}+\psi_{n-1}=[E(k)-V_n]\psi_n, \quad n=1,2,\cdots,L, \tag{4}$$

where k is the incident wave number and ψ_n is the wave function amplitude at the nth site. The on-site potential V_n for $1\leqslant n\leqslant L$ is independently and identically distributed with a box probability distribution, i.e., the V_n are uniformly distributed on the interval $[-\epsilon/2,\epsilon/2]$.

We open the sample by attaching one channel to the first site $n=1$. The Wigner delay time of a sample of length $n+1$ is then evaluated with the use of the Hamiltonian map approach[7] through the following iteration relations:

$$\tau_{n+1}=G_n^{-1}\left(\tau_n+\frac{1}{\sin k}\right)+\frac{A_n}{1+[\tan(\phi_n-k)+A_n]^2}\frac{\cot k}{\sin k},$$

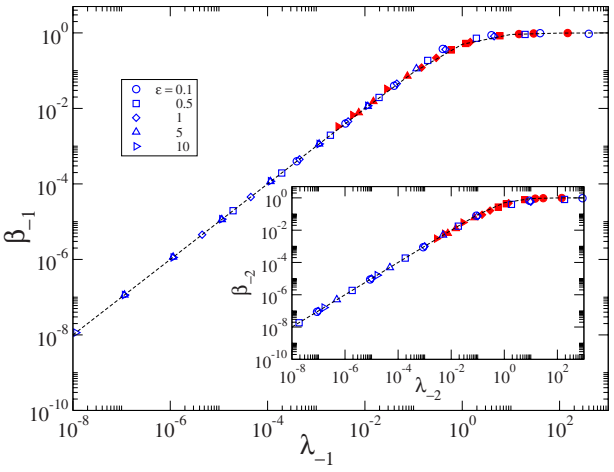

FIG. 1. (Color online) Scaled inverse delay times [Eq. (1)] for the Anderson model. Various symbols correspond to different disordered potentials $\epsilon\in\{0.1,0.5,1,5,10\}$ and $|E(k=\sqrt{\pi})|<1$. Blue hollow symbols denote delay time data for $q=1$. For comparison, red solid symbols denote $q'=2$ information length data, i.e., $l_L^{(q')}/L$ versus $\lambda=2l_\infty(\epsilon,E)/L$. The dashed line is the result of the best fit from Eqs. (12) and (13). Inset: same as in the main figure but now $q=2$ for delay times and $q'=3$ for information lengths.

$$G_n=1+A_n\sin[2(\phi_n-k)]+A_n^2\cos^2(\phi_n-k), \tag{5}$$

where $A_n=\frac{V_n}{\sin k}$, and the scattering phase is given by

$$\tan(\phi_{n+1})=\tan(\phi_n-k)+A_n. \tag{6}$$

In Fig. 1, we report the delay times for the Anderson model [Eq. (4)]. The data are averaged over an ensemble of 10^4 realizations of the random potential and are plotted according to the scaling [Eq. (1)]. The value of $\langle\tau_\infty^{-q}\rangle$ was calculated for a sample of length $L=10^7$, and its convergence was checked by increasing the system size by an additional order, i.e., $L=10^8$. The scaled data—for various L and disordered strengths ϵ—fall on a single curve, confirming the validity of the theoretical prediction [Eq. (1)]. Within the same figure, we also report the corresponding scaled entropic lengths (see solid red symbols) $l_L^{(q')}/L$ versus the localization parameter $\lambda=2l_\infty(\epsilon,E)/L$, in order to compare with the scaling law that dictates the delay times. The agreement between information lengths and delay times is evident, thus confirming that these two quantities are directly related. In the inset of Fig. 1, we also report our numerical results for the second moment, i.e., $q=2$. A nice agreement with the theoretical expectation [Eq. (1)] is again quite evident.

B. Microwaves propagating in a 1D waveguide

The creation of frequency pass and/or stop bands separated by mobility edges and their manipulation by imposing appropriate correlations in the disordered potential[26–31] have recently gained considerable research interest due to their immediate technological applications. One prominent theoretical suggestion[26] was based on the introduction of long-range correlations in the on-site disordered potential. The theoretical predictions were further supported by subsequent

experimental microwave measurements,[27] carried out in a single-mode waveguide with correlated scatterers realized by screws extending from a waveguide wall. By arranging the lengths of the screws according to a predefined sequence, correlated scattering arrangements could be realized leading to predefined mobility edges. If the screws are approximated by delta scatterers, the propagation of a single mode in the waveguide can be described by the wave equation for the Kronig-Penney model,

$$\psi''(z) + E\psi(z) = \sum_{n=-\infty}^{\infty} \epsilon_n \psi(z_n)\delta(z-nd), \tag{7}$$

where d is the distance between nearby scatterers, ψ is the electric field of the TE mode, and the energy is given by $E=k^2$. We can rewrite the above equation in the discrete form for $\psi_n \equiv \psi(z_n=nd)$,

$$\psi_{n+1} + \psi_{n-1} = [2\cos(kd) - U_n kd \sin(kd)]\psi_n. \tag{8}$$

One can split the potential U_n into a mean ϵ and a fluctuating term ϵ_n, $U_n=\epsilon+\epsilon_n$. Equation (8) is then equivalent to the tight-binding Eq. (4), with energy $E \to 2\cos k + k\epsilon \sin k$ and random potential $V_n \to k\epsilon_n \sin k$.

By choosing the on-site potential as[25,26]

$$\epsilon_n = \epsilon \sum_{m=-\infty}^{\infty} \xi_m \zeta_{n+m}, \tag{9}$$

where ζ_{n+m} is a random variable, uniformly distributed within the interval (0,1), and

$$\xi_m = \begin{cases} \sqrt{\dfrac{2}{\pi}}(\mu_2-\mu_1)^{3/2}, & m=0 \\ \dfrac{1}{m}\sqrt{\dfrac{\mu_2-\mu_1}{2\pi}}[\sin(2m\mu_2)-\sin(2m\mu_1)], & m\neq 0, \end{cases} \tag{10}$$

with $\mu_1=0.2\pi$, $\mu_2=0.4\pi$, and $\epsilon=-0.1$, it was argued that mobility edges can be tailored at wave numbers $kd/\pi=0.38$, 0.57, and 0.76. The experimental data[27] [see blue line (left axis) within the inset of Fig. 2 (Ref. 33)] did indeed seem to confirm the theoretical predictions. However, various questions still remain to be clarified—the most prominent being the nature of the corresponding eigenstates and how they are structurally affected by these potential correlations.

With the help of the iteration relations [Eqs. (5) and (6)], we have investigated the scaling properties of $\langle \tau_L^{-1} \rangle$ for the correlated model [Eqs. (7) and (9)]. Two energies E from both sides of the mobility edge $k=0.57\pi$ have been chosen. In Fig. 2, we report our numerical data by referring to the scaling variables β_{-1} and λ_{-1}, defined in Eq. (1). The data correspond to various system sizes $L \in 10^1, 10^2, \ldots, 10^6, 10^7$ and disordered strengths $\epsilon \in \{0.1, 0.5, 2.5, 5\}$. The remarkable agreement between the data from both sides of the "mobility" edge confirms again the theoretical prediction [Eq. (1)] and indicates clearly that the corresponding eigenfunctions have the same *structural* properties, thus being unaffected by the potential correlations. Using the scaling properties of the Wigner delay times, we are able to conclude that $k=0.57\pi$ does not correspond to any mobility edge separating extended from exponentially localized eigenstates. Rather, in both energy regimes, the eigenstates are structurally the same (i.e., exponentially localized), albeit the localization length is drastically different. This is reflected in the overall scaling factor $\langle \tau_\infty^{-1} \rangle$ [used to scale the data according to Eq. (1)], illustrated by the red circles (right axis) within the inset of Fig. 2. Note that $\tau_\infty \sim l_\infty$ (see, for example, Ref. 7). As we can see from Fig. 2, at the pass-band region, $\langle \tau_\infty^{-1} \rangle$ is much smaller than that of the stop-band region; i.e., l_∞ is much larger in the former case but nonetheless remains finite (a "true" transition would imply that $\langle \tau_\infty^{-1} \rangle \sim L^{-1}$, and thus by increasing the system size, the scaling factor had to go to zero). This abrupt change in the magnitute of $\langle \tau_\infty^{-1} \rangle$ around $k \sim 0.57\pi$ is a fingerprint of the correlations imposed to the disordered potential. Nevertheless, after rescaling the data, the universal scaling law [Eq. (1)] is again satisfied.

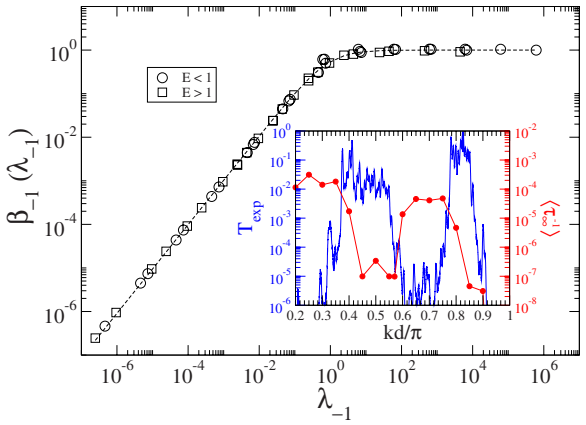

FIG. 2. (Color online) Scaled inverse delay times for microwaves propagating in 1D waveguide. The different symbols correspond to energies $|E(k=0.5\pi)|<1$, $|E(k=0.7\pi)|>1$ being on both sides of the critical wave vector $k=0.57\pi$. A nice data collapse is observed, indicating that in both cases, the statistical properties of delay times (and thus the structural properties of wave functions) are unaffected by the correlation and correspond to exponentially localized wave functions; albeit the localization length for $k=0.5\pi$ is much larger than for $k=0.7\pi$. This is reflected in the overall scaling parameter $\langle \tau_\infty^{-1} \rangle$. The dashed line is the result of the best fit from Eqs. (12) and (13). Inset: the experimental transmission coefficient showing pass and stop bands is displayed by the blue line (left axis). The values for $\langle \tau_{\text{inf}}^{-1} \rangle$ are shown by the red circles (right axis) (Ref. 33).

C. Disordered optical lattices

It was recently proposed in Ref. 34 that we can observe Anderson localization of ultracold atoms scattered off a gas of atoms of another species or internal state, randomly trapped at the nodes of an optical lattice. Within this setup, cooled vibrational ground-state atoms trapped at the nodes of a periodic optical lattice act as (static) delta scatterers provided that the kinetic energy of the incoming particles is less than the vibrational energy of the trapped scatterers, i.e., $\frac{\hbar^2 k^2}{2m_{\text{incoming}}} \ll \hbar\omega_{\text{scatterer}}$. The mathematical model that describes

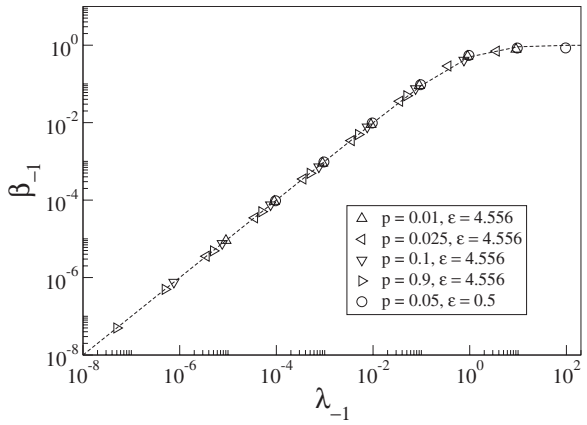

FIG. 3. Scaled inverse delay time for the disordered optical lattice system, with $\epsilon \in \{4.556, 0.5\}$ and filling factor $p \in \{0.01, 0.025, 0.05, 0.1, 0.9\}$. The nice data collapse confirms the universality of the scaling law [Eqs. (1) and (2)]. The dashed line is the result of the best fit from Eqs. (12) and (13).

the motion of the incoming particle along the lattice direction is the Kronig-Penney model [Eqs. (7) and (8)], in this case, with binary on-site potential distribution. Localization is then dependent on three parameters: wave vector k, disorder strength ϵ, and the filling factor $p \in [0,1]$. The latter dictates a binomial distribution of the on-site potential,

$$\epsilon_n = \begin{cases} \epsilon, & \zeta_n < p \\ 0, & \zeta_n \geq p, \end{cases} \tag{11}$$

where ζ_n is a random number given by a uniform distribution and ϵ is the disorder strength.[34] In the numerical simulations presented in Fig. 3, we used disorder strengths $\epsilon \in \{4.556, 0.5\}$ and filling factors $p \in \{0.01, 0.025, 0.05, 0.1, 0.9\}$. The larger disorder strength corresponds to numerical values used in Ref. 34. The very nice overlap of the scaled delay times is once more in excellent agreement with the universality of the scaling law [Eqs. (1) and (2)].

D. Universal behavior

It is illuminating to plot all our numerical data in the new variables,

$$Y_{-q} = \ln\left(\frac{\beta_{-q}}{1-\beta_{-q}}\right), \quad X_{-q} = \ln(\lambda_{-q}). \tag{12}$$

In these variables, the scaling for $q=1$ has an extremely simple form,

$$Y_{-1} = a_{-1} + b_{-1} X_{-1}, \tag{13}$$

with $a_{-1} \approx 0$ and $b_{-1} \approx 1$. The data for the scaling in variables Y_{-1}, X_{-1} are presented in Fig. 4. The remarkable result is that the above simple scaling relation holds in a very large region

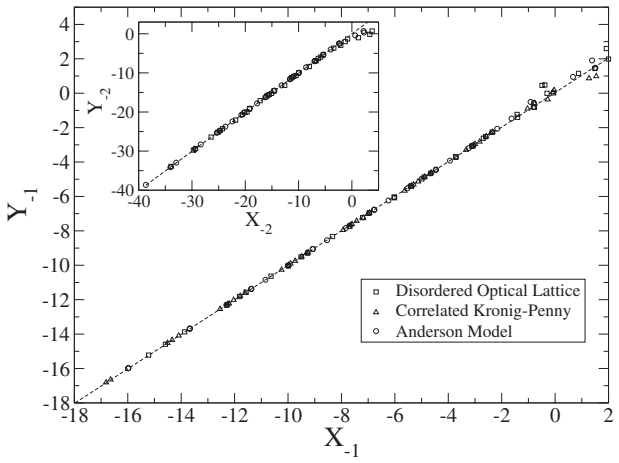

FIG. 4. Scaling of Eqs. (1) and (2) in the variables from Eq. (12). Inset: same as in the main figure but now for the $q=2$ case.

of the scaling parameter, $\Delta X_{-1} \approx 14$. In fact, Eq. (13) is exact only for $q=1$, corresponding to $q'=2$.[15,16] However, for other values of q, Eq. (13) is still a good approximation (see the inset of Fig. 4 for the case $q=2$). Placing Eq. (12) into Eq. (13), we find that $\frac{\beta_{-1}}{1-\beta_{-1}} = \lambda_{-1}$ (see the dashed lines in Figs. 1–3). This takes the form (2) once we substitute for β_{-1} and λ_{-1} the expressions in Eq. (1). In the inset of the same figure, we also report the $q=2$ moment of delay times by making use of the variables of Eq. (12). The nice data collapse reconfirms the validity of Eq. (13) where again $a_{-2} \approx 0$ and $b_{-2} \approx 1$ (note, however, that for $q=2$, small deviations from the straight line are evident around $X_{-2} \approx 0$).

III. CONCLUSIONS

In conclusion, we have investigated the scaling properties of inverse moments of Wigner delay times. We have shown that they are dictated by the scaling law [Eq. (1)], which can be rewritten in a more familiar way [Eq. (2)], resembling the scaling relation for the information lengths of wave function components. Our theoretical arguments have been tested in various physical models where the applicability of the nonlinear σ model is questionable, thus strongly supporting the relation between wave function moments and inverse moments of Wigner delay times.

ACKNOWLEDGMENTS

T.K. and J.D.B. acknowledge an Academic Excellence grant from SUN and thank greatly Ulrich Kuhl for the inset data of Fig. 2, as well as insightful discussions. J.A.M.-B. thanks support from project CB-2006-01-60879, CONACyT Mexico. Computer time at Wesleyan University supported by the NSF under Grant No. CNS-0619508. This research was supported by a grant from the United States–Israel Binational Science Foundation (BSF), Jerusalem, Israel.

[1] Y. V. Fyodorov and H.-J. Sommers, J. Math. Phys. **38**, 1918 (1997); Y. V. Fyodorov, D. V. Savin, and H.-J. Sommers, J. Phys. A **38**, 10731 (2005).
[2] K. J. H. van Bemmel, H. Schomerus, and C. W. J. Beenakker, Phys. Scr., T **T90**, 278 (2001).
[3] A. Z. Genack, P. Sebbah, M. Stoytchev, and B. A. van Tiggelen, Phys. Rev. Lett. **82**, 715 (1999).
[4] A. A. Chabanov and A. Z. Genack, Phys. Rev. Lett. **87**, 233903 (2001).
[5] J. Pearce, Z. Jian, and D. M. Mittleman, Phys. Rev. Lett. **91**, 043903 (2003); Z. Jian, J. Pearce, and D. M. Mittleman, *ibid.* **91**, 033903 (2003).
[6] H. Schomerus, K. J. H. van Bemmel, and C. W. J. Beenakker, Europhys. Lett. **52**, 518 (2000); Phys. Rev. E **63**, 026605 (2001); H. Schomerus, *ibid.* **64**, 026606 (2001).
[7] A. Ossipov, T. Kottos, and T. Geisel, Phys. Rev. B **61**, 11411 (2000).
[8] C. Texier and A. Comtet, Phys. Rev. Lett. **82**, 4220 (1999); C. J. Bolton-Heaton, C. J. Lambert, V. I. Falko, V. Prigodin, and A. J. Epstein, Phys. Rev. B **60**, 10569 (1999).
[9] Y. V. Fyodorov, JETP Lett. **78**, 250 (2003).
[10] Tsampikos Kottos, J. Phys. A **38**, 10761 (2005).
[11] A. Ossipov and Y. V. Fyodorov, Phys. Rev. B **71**, 125133 (2005).
[12] A. D. Mirlin, Y. V. Fyodorov, A. Mildenberger, and F. Evers, Phys. Rev. Lett. **97**, 046803 (2006).
[13] J. A. Méndez-Bermúdez and T. Kottos, Phys. Rev. B **72**, 064108 (2005); M. Weiss, J. A. Méndez-Bermúdez, and T. Kottos, *ibid.* **73**, 045103 (2006); J. A. Méndez-Bermúdez and I. Varga, *ibid.* **74**, 125114 (2006).
[14] T. Kottos and M. Weiss, Phys. Rev. Lett. **89**, 056401 (2002); F. Steinbach, A. Ossipov, T. Kottos, and T. Geisel, *ibid.* **85**, 4426 (2000).
[15] Y. V. Fyodorov and A. D. Mirlin, Int. J. Mod. Phys. B **8**, 3795 (1994).
[16] Y. V. Fyodorov and A. D. Mirlin, Phys. Rev. Lett. **69**, 1093 (1992); A. D. Mirlin and Y. V. Fyodorov, J. Phys. A **26**, L551 (1993).
[17] G. Casati, I. Guarneri, F. Izrailev, S. Fishman, and L. Molinari, J. Phys.: Condens. Matter **4**, 149 (1992).
[18] B. L. Altshuler, V. E. Kravtsov, and I. V. Lerner, in *Mesoscopic Phenomena in Solids*, edited by B. L. Altshuler, P. A. Lee, and R. A. Webb (North Holland, Amsterdam, 1991).
[19] B. A. Muzykantskii and D. E. Khmelnitskii, Phys. Rev. B **51**, 5480 (1995).
[20] V. I. Falko and K. B. Efetov, Europhys. Lett. **32**, 627 (1995); Phys. Rev. B **52**, 17413 (1995).
[21] A. D. Mirlin, J. Math. Phys. **38**, 1888 (1997); Phys. Rep. **326**, 259 (2000); *Proceedings of the International School of Physics "Enrico Fermi" Course CXLIII*, edited by G. Casati, I. Guarneri, and U. Smilansky (IOS, Amsterdam, 2000).
[22] I. E. Smolyarenko and B. L. Altshuler, Phys. Rev. B **55**, 10451 (1997).
[23] V. M. Apalkov, M. E. Raikh, and B. Shapiro, Phys. Rev. Lett. **89**, 126601 (2002).
[24] A. Ossipov, T. Kottos, and T. Geisel, Phys. Rev. E **65**, 055209(R) (2002); T. Kottos, A. Ossipov, and T. Geisel, *ibid.* **68**, 066215 (2003).
[25] U. Kuhl, F. M. Izrailev, and A. A. Krokhin, arXiv:0709.1355 (unpublished).
[26] F. M. Izrailev and A. A. Krokhin, Phys. Rev. Lett. **82**, 4062 (1999).
[27] U. Kuhl, F. M. Izrailev, A. A. Krokhin, and H.-J. Stöckmann, Appl. Phys. Lett. **77**, 633 (2000); A. Krokhin, F. Izrailev, U. Kuhl, H.-J. Stöckmann, and S. E. Ulloa, Physica E (Amsterdam) **13**, 695 (2002).
[28] D. H. Dunlap, H.-L. Wu, and P. W. Phillips, Phys. Rev. Lett. **65**, 88 (1990); P. W. Phillips and H.-L. Wu, Science **252**, 1805 (1991); F. M. Izrailev, T. Kottos, and G. P. Tsironis, Phys. Rev. B **52**, 3274 (1995).
[29] F. A. B. F. de Moura and M. L. Lyra, Phys. Rev. Lett. **81**, 3735 (1998); H. Shima, T. Nomura, and T. Nakayama, Phys. Rev. B **70**, 075116 (2004); P. Carpena, P. Bernaola-Galván, P. Ch. Ivanov, and H. E. Stanley, Nature (London) **418**, 955 (2002); P. Carpena, P. Bernaola-Galván, and P. Ch. Ivanov, Phys. Rev. Lett. **93**, 176804 (2004).
[30] V. Bellani, E. Diez, R. Hey, L. Toni, L. Tarricone, G. B. Parravicini, F. Domínguez-Adame, and R. Gómez-Alcalá, Phys. Rev. Lett. **82**, 2159 (1999).
[31] A. Rodriguez, V. A. Malyshev, G. Sierra, M. A. Martín-Delgado, J. Rodríguez-Laguna, and F. Domínguez-Adame, Phys. Rev. Lett. **90**, 027404 (2004); J. Phys. A **33**, L161 (2000); A. V. Malyshev, V. A. Malyshev, and F. Domínguez-Adame, Phys. Rev. B **70**, 172202 (2004).
[32] M. Titov and H. Schomerus, Phys. Rev. Lett. **95**, 126602 (2005).
[33] We are grateful to Dr. U. Kuhl for providing us the experimental curve shown in the inset of Fig. 2.
[34] U. Gavish and Y. Castin, Phys. Rev. Lett. **95**, 020401 (2005).
[35] E. P. Wigner, Phys. Rev. **98**, 145 (1955); F. T. Smith, *ibid.* **118**, 349 (1960).
[36] C. A. A. de Carvalho and H. M. Nussenzveig, Phys. Rep. **364**, 83 (2002).